Available online at www.sciencedirect.com
ScienceDirect
Ceramics International 35 (2009) 755–762
CERAMICS INTERNATIONAL
www.elsevier.com/locate/ceramint

Preparation of zirconium tungstate (ZrW_2O_8) by the amorphous citrate process

C. Georgi *, H. Kern

Technische Universität Ilmenau, Institut für Werkstofftechnik, Gustav-Kirchhoff-Str. 6, D-98693 Ilmenau, Germany

Received 19 December 2007; received in revised form 17 January 2008; accepted 10 February 2008
Available online 4 June 2008

Abstract

Citrate gels were prepared from aqueous solutions of zirconium dinitrate oxide, ammonium metatungstate and citric acid in the range of pH 1.1–10. The citric acid to total metal molar ratio was varied from 0.66 to 1.33. The thermal decomposition of these precursor gels and the oxide phase evolution were studied by thermal analysis (DTA, TG, EGA-MS) and X-ray powder diffraction (XRD), respectively. Complex stability appeared to be largely insensitive to pH variations, whereas consistency and thermal behaviour of the gels were found to be influenced by pH and molar ratio of the starting solutions. Under optimized thermolysis conditions, phase-pure trigonal ZrW_2O_8 was obtained which was converted to cubic ZrW_2O_8 by up-quenching to 1125 °C for a very short time (<1 min). The cubic ZrW_2O_8 has particle sizes in the lower micron to submicron range and shows a negative linear coefficient of thermal expansion CTE = -10.2×10^{-6} K^{-1} (30–120 °C). The polymorphism of ZrW_2O_8 is discussed with respect to its preparation by the amorphous citrate process and other soft chemistry routes.

Keywords: A. Sol–gel processes; C. Thermal expansion; ZrW_2O_8

1. Introduction

Zirconium tungstate ZrW_2O_8 exhibits negative thermal expansion (NTE) based on correlated motions of its polyhedral structure units (''rigid unit modes'') [1,2]. It has a high negative thermal expansion coefficient over its entire stability range [3], and the NTE is isotropic because the crystal structure [4] is cubic. NTE-materials have potential applications in compensating for the positive thermal expansion behaviour of other materials, for instance in composites with controlled thermal expansion characteristics [5,6]. Such applications have brought about a need for ZrW_2O_8 powders of high quality with regard to phase purity and particle size.

Although ZrW_2O_8 is thermodynamically stable only from 1105 °C to 1257 °C [7], it can be quenched to room temperature and then remains kinetically stable on heating to about 770 °C [3]. Synthesis of ZrW_2O_8 by the solid state reaction between ZrO_2 and WO_3 requires several days of heating at about 1200 °C [7] and is further complicated by the volatilization of WO_3 at high temperatures [3]. Several low-temperature soft chemistry routes have been reported for ZrW_2O_8 including dehydration of hydrothermally crystallized basic zirconium tungstate [8,9], non-hydrolytic sol–gel synthesis [10–12] and solution combustion [9]. Despite successes achieved with these routes, there are some drawbacks like multi-day synthesis procedures [10], moisture sensitivity of the reagents [12], and phase separation into equilibrium phases [9] which limit their applicability for powder synthesis.

A very effective solution-based technique is the amorphous citrate process (ACP) [13,14] in which the homogeneity of an aqueous solution of metal citrate complexes is preserved in an amorphous gel and into the final solid oxide product. Maximum homogeneity of cation distribution may be achieved when a heterometallic complex with the desired stoichiometry is utilized rather than the individual metal complexes [15]. In order to take full advantage of this technique, it is essential to maintain cation homogeneity during the whole process prior to oxide formation, including solution concentration and gel thermolysis. Therefore, complex stability is of vital interest. Polydentate molecules like citric acid (CA) are known to form very stable chelates in particular with transition metal ions [16]. Citrate complexes of both zirconium and tungsten have been

* Corresponding author. Tel.: +49 3677 693284; fax: +49 3677 691597.
E-mail address: christian.georgi@tu-ilmenau.de (C. Georgi).

0272-8842/$34.00
doi:10.1016/j.ceramint.2008.02.010

reported in the literature [17–19]. It is assumed that CA coordinates to the metal atom in bidentate mode by the deprotonated oxygens of the central OH group and of the vicinal carboxylate group. The uncomplexed carboxylate groups of CA form ionic crosslinks with metal centers of adjacent complexes [19,20] constituting a highly viscous liquid, which is commonly referred to as citrate gel [15].

Though the ACP evidently has the potential for cation mixing at the molecular scale and, thus, for the direct crystallization of metastable polymetallic oxides at low homologous temperatures, it has, to the best of our knowledge, not yet been employed to synthesize ZrW_2O_8 (de Buysser et al. [21] limited themselves to the preparation of an oxide mixture of ZrO_2 and WO_3 for the subsequent ceramic processing of ZrW_2O_8).

This paper presents an investigation of the synthesis of zirconium tungstate by the ACP with the overall aim to develop a relatively simple and efficient preparation method for phase-pure cubic powders of small particle size.

2. Experimental procedure

2.1. Synthesis

The starting materials were zirconium dinitrate oxide $ZrO(NO_3)_2{\cdot}xH_2O$ (99.9%, Alfa Aesar) and ammonium metatungstate $(NH_4)_6W_{12}O_{39}{\cdot}xH_2O$ (99.98%, H.C. Starck). Because of the undefined content of crystal water in both compounds, weighed amounts of each of them were heated to 900 °C and 600 °C, respectively, for conversion to ZrO_2 and WO_3. The observed weight losses were then used to calculate exact amounts of zirconium dinitrate oxide and ammonium metatungstate to be used to prepare aqueous solutions containing known amounts of Zr or W. First, two single solutions of the respective metal salts were prepared which, when mixed, gave a solution containing Zr and W in the stoichiometric ratio of ZrW_2O_8. These solutions were 0.1 M with respect to the metal. Then, anhydrous CA (99.5%, Alfa Aesar) was added under constant stirring to the zirconium dinitrate oxide solution in a molar proportion CA to metal of 2:1. A white precipitate immediately formed, which redissolved after some minutes. The amount of CA added to the ammonium metatungstate solution was varied in such a way that molar ratios of CA to total metal cations of 1.33, 1 and 0.66 were realized after mixing the individual solutions. The pH of the mixed solution was measured to lie between 1.1 and 1.2 and is referred to as ''natural pH'' (pH_{nat}) in this paper. The pH was varied up to pH 10 by adding aqueous ammonia solution (25%, p.a., Merck). It was not increased further beyond pH 10 because of strong ammonia evolution during the subsequent concentration of the solution. The clear and colourless solution was concentrated in a rotary evaporator under vacuum at 70 °C until the viscosity was still low enough to empty the flask. The concentrated solution was then poured into dishes and dried for 20 h at 85 °C. Thermolysis of the obtained gels was performed in a muffle furnace with vented heating chamber using different heating schemes (for details see Section 3.2). Finally, some experiments were performed in order to obtain both mono-metallic and ammonium citrate gels in an analogous way by omitting the non-required compounds.

2.2. Characterization

Differential thermal analysis (DTA) and thermogravimetry (TG) were carried out in order to study the thermolysis process using a simultaneous thermal analyzer (STA 409 EP, Netzsch). Samples of 25 mg were heated at a rate of 10 °C/min in a Pt crucible in static air. Evolved gas analysis by means of mass spectrometry (EGA-MS) was performed on selected samples using a Netzsch Aeolus® system fitted with a simultaneous thermal analyzer (STA 449C, Netzsch) by a heated capillary (carrier gas air at a flow rate of 70 ml/min). X-ray diffraction (XRD) was used to analyze phase evolution at various stages of synthesis. A diffractometer (D8 Advance, Bruker AXS) with Co-K_α radiation and Bragg–Brentano focussing geometry was employed. Variable temperature XRD data were collected on a diffractometer (ID 3003, Seifert) equipped with an heating attachment (XRK 900, Anton Paar). The morphology of the products was examined using a scanning electron microscope (XL30, FEI).

3. Results and discussion

3.1. Complexation and gel formation

Fig. 1 provides a survey of the Zr–W-citrate gels prepared in this study. Two findings are especially noteworthy. First, complex stability appears to be largely insensitive to pH variations, no precipitation was observed up to pH 10. By contrast, $Zr(OH)_4$ precipitates in the Zr^{4+}–CA–water system above pH 7 when $[Zr^{4+}] = 0.1$ M [18]. Therefore, single metal Zr–CA-complexes seem to be unlikely to occur in the Zr–W-citrate solutions. Second, the case of CA-deficient gels (molar ratio 0.66) indicates that other than simple equimolar metal citrate complexes must be considered under the present

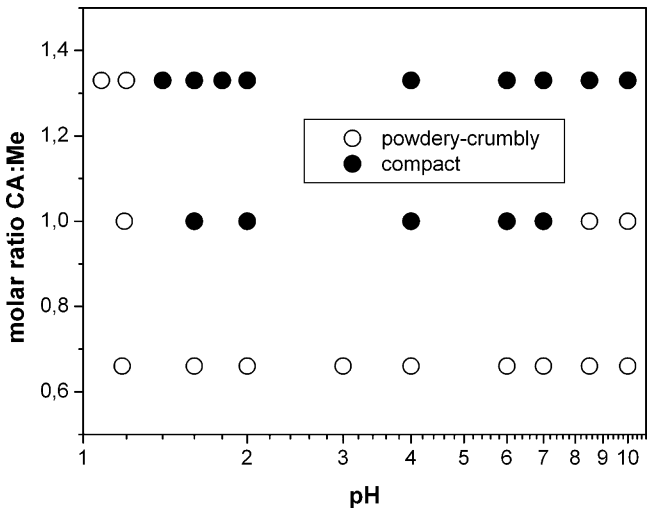

Fig. 1. Survey of gels prepared in this study. Different kinds of gel consistency are indicated.

conditions. In a study on the preparation of perovskites by the amorphous citrate process, Baythoun and Sale [22] proposed structural arrangements of heterometallic complexes with molar ratios <1. Though a detailed analysis of the complex chemistry in the system Zr–W–CA is beyond the scope of this report, it is our belief that these two findings support the idea of heterometallic complex formation. Further indirect evidence of heterometallic complexation is discussed in Section 3.2.

The as-prepared gels are X-ray amorphous and present no microscopic evidence of inhomogeneity except for uniformly dispersed fine gas bubbles in gels with pH ≤2. The vitreous material is transparent and uniformly coloured. The colour of the gels varies from colourless to smoky and pale yellow. Regarding their consistency, the brittle gels can be classified either as compact or as powdery crumbly (Fig. 1), a distinction which reflects different drying behaviour. During drying, stresses develop in constrained gels, thus leading to cracking and disintegration unless the material has the capacity to release stress. Gel properties like shape sustainability and elasticity are affected by the nature and the density of crosslinking. Thus, the observed differences in gel consistency must be related to the influence of pH and CA-concentration (here expressed as molar ratio of CA to total metal cations) on ionic crosslinking. CA is a tricarboxylic acid with acid dissociation constant (pK_a) values between 3 and 6 [23]. Depending on the pH of the solution, the uncomplexed carboxyl groups are dissociated to a different extent. Moreover, it has to be taken into account that the adjustment of the pH by the addition of ammonia brings about an increase in the concentration of NH_4^+ ions and that in the presence of these ions ammonium-carboxylate bridges can be formed in carboxylate gels [20]. This means that the increasing deprotonation of CA in combination with the supply of an additional crosslinker (NH_4^+) leads to the formation of ammonium-carboxylate crosslinks, which obviously make gels more resistant to disintegration (compact gels). At pH ∼1, CA is almost fully protonated, the crosslink density at pH_{nat} is therefore low, resulting in powdery crumbly gels for all CA-concentrations. At pH ∼7, the deprotonation of CA is nearly complete. Therefore, in the range $pH_{nat} < pH \leq 7$ compact gels

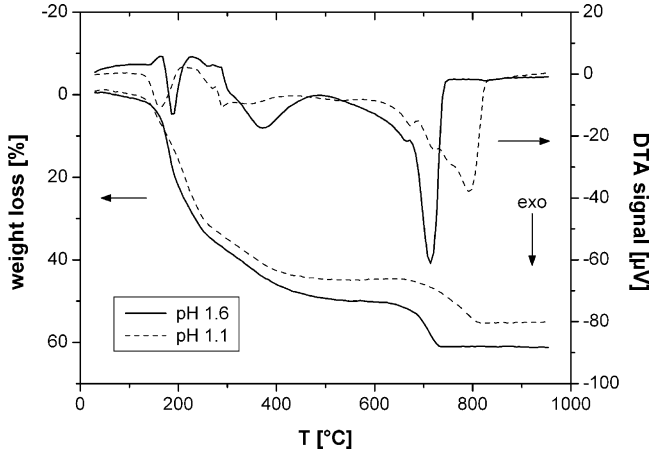

Fig. 2. TG–DTA curves for a gel prepared with a molar ratio 1.33 at pH 1.6 (for comparison, the traces of the corresponding gel with pH_{nat} are also plotted).

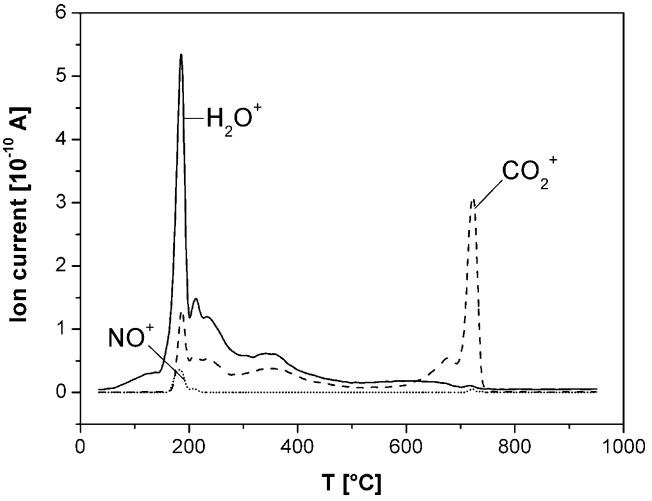

Fig. 3. EGA-MS profiles for a gel prepared with a molar ratio 1.33 at pH 1.6.

are expected. This is, indeed, observed for molar ratios of 1 and 1.33. A further increase beyond pH 7 for solutions of molar ratio 1 leads to powdery crumbly gels, probably because the ions introduced by the addition of ammonia now do not take part in crosslinking but weaken the ionic interactions through a shielding effect [24]. If there is an excess of CA (molar ratio 1.66), gel-forming ionic interactions can proceed between NH_4^+ and carboxylate groups of non-chelating CA. (In auxiliary experiments we prepared ammonium citrate gels from CA and ammonia in the range $3 \leq pH \leq 10$.) Thus, for gels of molar ratio 1.66 compact gels are obtained from pH 1.4 up to pH 10. Gels with a CA deficiency (molar ratio 0.66) can build up ammonium-carboxylate crosslinks only to a limited extent and are powdery crumbly over the entire pH range.

3.2. Gel thermolysis

In the ACP, oxide phase formation is brought about by the complete thermal decomposition of the citrate complex gels. Hence, it is important to maintain the cation homogeneity during the entire thermal treatment. To set up an appropriate heating regime for the crystallization of ZrW_2O_8 (see Section 3.3), gel thermolysis was studied by thermal analysis. DTA and TG traces of the gels prepared in the range $1.4 \leq pH \leq 10$ were found to be very similar for all molar ratios, which indicates that the chelated metal cations become almost insensitive to pH variations in wide acidity ranges. Therefore, thermolysis is exemplified here by a gel with pH 1.6 and molar ratio 1.33 (Figs. 2 and 3).

Two basic stages of decomposition associated with strong exotherms and distinctive weight losses can be discerned. The first stage ranges from 100 °C to 500 °C, the second one from 600 °C to 750 °C (approximate temperatures). Both stages are separated by a region without marked thermal effects between 500 °C and 600 °C. The EGA-MS profiles (Fig. 3) for *m/e* values of 18 (H_2O^+), 30 (NO^+) and 44 (CO_2^+ and N_2O^+) show that the initial weight loss and the DTA exotherm at about 190 °C occur as a result of oxidative decomposition and

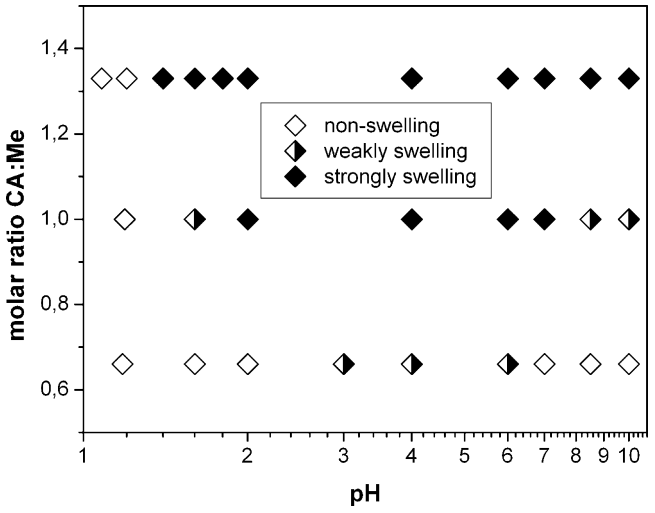

Fig. 4. Swelling behaviour of Zr–W-citrate gels.

dehydration of the gel. At temperatures above 200 °C, the decomposition proceeds and comes to a halt at approximately 500 °C. At around 600 °C, the signal for *m/e* 44 increases culminating in a large peak at 720 °C, which corresponds to a strong DTA exotherm and the final weight loss at this temperature. The *m/e* 44 peak can be assigned to CO_2^+ because there is only a negligible small signal for *m/e* 30 (NO^+) at 720 °C (NO^+ ions occur as a cracking fragment of N_2O^+ ions). Hence, the effects at 720 °C are caused by the elimination of carbon. Note that the final exotherm is shifted from 800 °C to 720 °C by changing the pH of the starting solution from 1.1 to 1.6 (Fig. 2). For gels prepared in the range $1.4 \leq pH \leq 10$, this exotherm is found at temperatures between 710 °C and 740 °C.

To study the first stage of thermolysis in more detail, samples of the gels compared in Fig. 2 were heated at 10 °C/min to 500 °C and removed from the oven for inspection at different temperatures. The gel with pH 1.6 begins to soften at 150 °C, at 190 °C a swollen brittle brownish mass is formed. Further heating to 500 °C turns the material into a black char, leaving its voluminous shape unchanged. By contrast, the gel prepared at pH_{nat} is transformed by this thermal treatment into a powdery crumbly black char without any indication of deformation. Both gels show comparable weight losses due to gas evolution at the first stage of thermolysis (Fig. 2). Hence, softening must be responsible for their completely different swelling behaviour: swelling occurs only when gases escape from a softened gel. The subsequent examination of all prepared gels (Fig. 4) revealed that their swelling behaviour varies with the preparation conditions in an analogous way as gel consistency does. Like gel consistency, gel softening (and therefore gel swelling) is affected by the nature and the density of the crosslinks which, in turn, are strongly influenced by pH and CA-concentration (*vide supra*). Gels prepared at pH_{nat} do not swell. CA-deficient gels with a molar ratio 0.66 swell weakly in the range $3 \leq pH \leq 6$ where dissociated carboxylate species are predominant. For a molar ratio of 1 strong swelling is observed in the range $2 \leq pH \leq 7$, whereas weakening of crosslinking for pH >7 yields only slightly swelling gels. In the case of excess CA (molar ratio 1.33), strongly swelling gels are obtained from pH 1.4 up to pH 10.

Regarding the cation homogeneity prior to oxide crystallization, it is of some interest to deal with the implications of heterometallic complex formation (see Section 3.1). For this purpose, we compared Zr–W-citrate gels with the corresponding monometallic citrate gels with respect to their thermal stability. As can be seen from Fig. 5, oxide crystallization occurs at 500 °C both in the Zr- and in the W-gel, respectively, while an X-ray amorphous product results from the Zr–W-gel at this temperature. Thus, the behaviour of heterometallic gels cannot be interpreted in terms of a simple addition of the monometallic gels. This observation suggests the formation of a stable heterometallic Zr–W–CA-complex under the present experimental conditions, which prevents phase separation during gel thermolysis.

Summing up the results of thermal analysis, the following mechanism of thermolysis can be stated for gels prepared in the range $1.4 \leq pH \leq 10$. The first stage (100–500 °C) involves the scission of ionic crosslinks, the dehydration of the gel and the oxidative decomposition of carboxylate groups except for carboxylates coordinated to metals. Swelling occurs depending on pH and CA-concentration. At 500 °C, an amorphous black char with no indication of phase separation is formed. After an intermediate stage without marked thermal events (500–600 °C), the complete breakdown of the metal-carboxylate bonds occurs concomitantly with oxide crystallization in the second stage (600–750 °C).

3.3. Oxide crystallization

Thermal treatments to obtain crystalline ZrW_2O_8 were initially carried out by heating ~1 g of the powdered gel in a platinum boat at a rate of 10 K/min to 740 °C and holding it at this temperature for 30 min. In the following, this procedure is referred to as "conventional heat treatment". XRD patterns

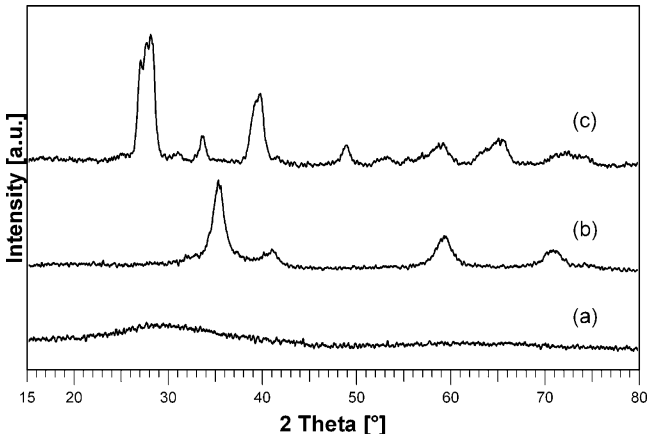

Fig. 5. XRD patterns of thermolysis products of heterometallic (a) and monometallic (b and c) gels. The gels were heated for 1 h at 500 °C and then removed from the oven. (a) Amorphous product from a Zr–W-citrate gel. (b) Tetragonal ZrO_2 (PDF number 50-1089) from a Zr-citrate gel. (c) Orthorhombic WO_3 (PDF number 71-131) from a W-citrate gel. All gels were prepared from solutions of pH 2, molar ratios were 1.33 (a), 2 (b) and 1 (c).

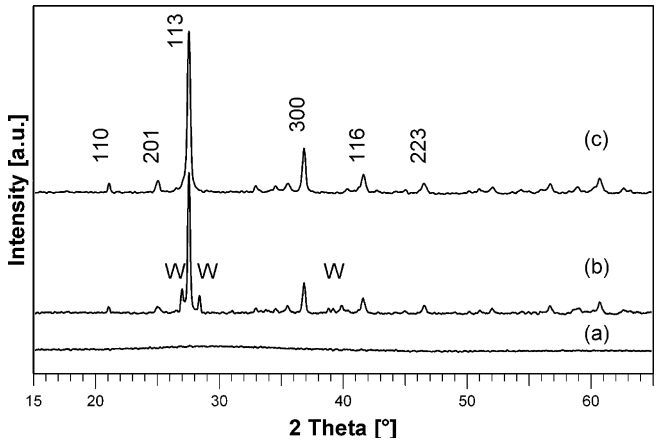

Fig. 6. XRD patterns for various heat treatments (for details see text) of a Zr–W-citrate gel (pH 1.6, molar ratio 1.33). (a) 600 °C, conventional; (b) 740 °C, conventional; (c) 740 °C, optimized. Reflections of monoclinic WO_3 (PDF number 83-950) are marked by W, all other peaks belong to t-ZrW_2O_8. The main peaks of t-ZrW_2O_8 are indexed in (c).

showing the phase evolution of a gel with pH 1.6 and molar ratio 1.33 on heating are shown in Fig. 6. At 600 °C, a black char, which is still X-ray amorphous (Fig. 6a) was obtained, thus confirming the intermediate stage of thermolysis between 500 °C and 600 °C found by thermal analysis. While it was not possible to identify the phase(s) crystallizing at 740 °C on the basis of the powder diffraction file [25], the diffraction pattern (Fig. 6b) was found to be very similar to the one reported by Wilkinson et al. [11] for trigonal zirconium tungstate (t-ZrW_2O_8). The light yellow colour of the porous mass indicated the formation of WO_3, which was confirmed by some weak reflections of monoclinic WO_3 in the XRD pattern (Fig. 6b). We therefore concluded that the conventional heat treatment led to the crystallization of t-ZrW_2O_8 along with minor amounts of the binary oxides WO_3 and ZrO_2. However, under the thermolysis conditions of the ACP, we never observed the monoclinic equilibrium phase of ZrO_2 (baddeleyite). This is presumably due to the formation of a tetragonal ZrO_2 (see the monometallic gel in Fig. 5b), whose amount is too small to be detected by XRD. Traces of WO_3 were found in the inner material of the mass even for short dwelling times (∼1 min) at 740 °C. Phase separation into equilibrium phases occurs due to self-heating by the strong final exothermic reaction and is a common problem in the thermolysis of carboxylate gels [26,27]. Moreover, strong residues of unburnt matter were observed at the bottom of the boat for dwelling times shorter than 30 min. This low decomposition rate results from stagnant layer formation due to the tall side walls (10 mm) of the boat. Hence, for the preparation of a phase-pure product the heat treatment procedure had to be optimized with regard to heat and mass transfer.

Various heating schemes (including two-stage firing and up-quenching) and gel bed/crucible geometries were tested. These experiments along with the results of thermal analysis eventually led to the following optimized heat treatment: gel pieces (∼1 g) of 1–2 mm diameter were spread in a thin layer on a free-standing platinum net (mesh width 0.75 mm). During the first and the intermediate stage of thermolysis (20–620 °C), the gel was rapidly heated (∼20 K/min), whereas at the second stage heating to 740 °C was performed at a rate of ∼7 K/min. After holding at 740 °C for 1 min, the sample was removed from the oven. This optimized heat treatment yields a white voluminous mass which shows no reflections of WO_3 in its powder diffraction pattern (Fig. 6c).

Though the crystal structure of t-ZrW_2O_8 has not been solved yet, it has been shown [11,12] that its diffraction pattern can be indexed on the basis of an expanded cell (a, $1.5c$) of the trigonal $ZrMo_2O_8$ structure [28]. Using the program PowderX [29], we found that all reflections of the observed pattern (Fig. 6c) can be indexed on a trigonal cell with $a = 9.80$ Å and $c = 17.60$ Å. Thus, the product of the optimized heat treatment is metastable trigonal zirconium tungstate, which is virtually free from equilibrium phases according to the absence of WO_3-reflections in the XRD pattern (from here on called "phase-pure t-ZrW_2O_8").

The results of the optimized heat treatment procedure for all gels prepared in this study are presented in Fig. 7. As can be seen, phase-pure t-ZrW_2O_8 can be prepared over a wide range of solution pH and molar ratio CA:Me. Comparative inspection of Figs. 4 and 7 reveals that the phase purity of the oxide is favourably influenced by the swelling of the gel. Swelling creates a large surface for effective heat and mass transfer, thus incomplete thermolysis and phase separation by local overheating are largely avoided. Despite their swelling, gels with a molar ratio of 1.33 and pH ≥ 7 exhibit phase separation. This may be attributed to the formation of amorphous ammonium citrate from NH_4^+ ions and excess (non-chelating) CA (see Section 3.1). We found that the thermolysis of ammonium citrate gels does not end before a temperature of 650 °C is reached, whereas the thermal decomposition sequence of CA is complete at temperatures around 250 °C. These findings are in

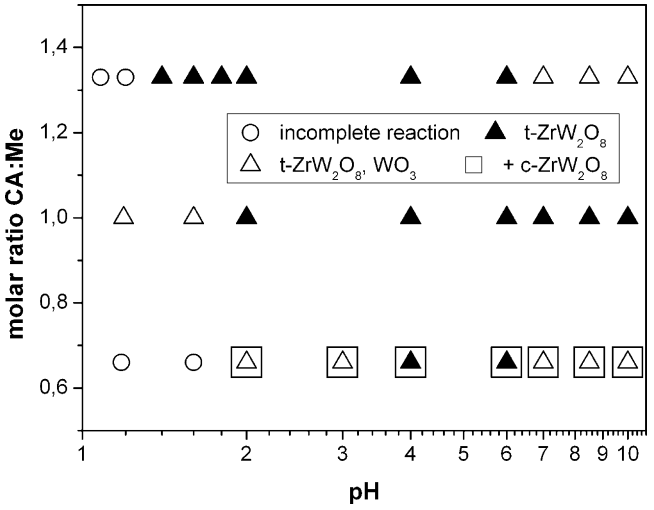

Fig. 7. Oxide phases obtained by the optimized heat treatment. The symbol (▲) denotes phase-pure t-ZrW_2O_8 according to the absence of the strongest reflection (200 at 28.37°2θ) of monoclinic WO_3 in the XRD pattern. Products consisting of t-ZrW_2O_8 with minor contents of WO_3 are marked by (△). Samples in which c-ZrW_2O_8 was detected in the XRD pattern according to $I_{0\,1\,2}$ (cubic) > $I_{2\,0\,1}$ (trigonal) are additionally marked by (□).

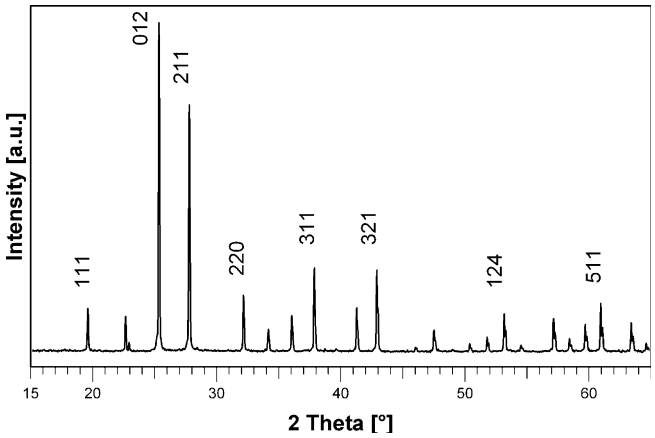

Fig. 8. XRD pattern of c-ZrW_2O_8 obtained by up-quenching t-ZrW_2O_8 to 1125 °C. All reflexes match PDF 50-1868 for c-ZrW_2O_8 (main peaks are indexed).

accordance with the results of van Werde et al. [30]. Thus, the exothermic decomposition of ammonium citrate interferes with the thermolysis of the Zr–W-citrate gel up to 650 °C and may lead to overheating and segregation.

3.4. Conversion of trigonal into cubic zirconium tungstate

In Section 3.3, it was shown that under optimized conditions of the ACP the formation of the equilibrium phases ZrO_2 and WO_3 can be kinetically suppressed and trigonal ZrW_2O_8 is obtained. Hence, at ambient to low temperatures ($T < 750$ °C), two metastable polymorphs of zirconium tungstate (cubic and trigonal) can exist. As the aim of this study was to prepare phase-pure cubic zirconium tungstate, two questions arise: (i) Can the phase formation of ZrW_2O_8 be influenced by synthesis conditions? and (ii) Can t-ZrW_2O_8 be converted into c-ZrW_2O_8 at low temperatures?

As far as these questions are concerned, we made the following observations. At $T = 740$ °C, minor but distinct contents of c-ZrW_2O_8 result only from gels with a molar ratio of 0.66 (Fig. 7) according to the X-ray intensity relation $I_{0\,1\,2}$ (cubic) $> I_{2\,0\,1}$ (trigonal). Gel thermolysis at temperatures $T \geq 770$ °C generally leads to gradual decomposition into the binary oxides until t-ZrW_2O_8 has completely disappeared at ~840 °C. When t-ZrW_2O_8 is up-quenched to 920 °C, c-ZrW_2O_8 is formed, but always along with WO_3 and (tetragonal) ZrO_2. The trigonal phase cannot be converted into c-ZrW_2O_8 by prolonged heating, it decomposes at 700 °C to the binary oxides within 24 h. These observations are consistent with the results of other attempts to synthesize zirconium tungstate by solution methods [11,12]. Which polymorph can be obtained using a given synthesis method depends on both thermodynamic and kinetic factors. t-ZrW_2O_8 obviously is thermodynamically more stable than c-ZrW_2O_8 in the low T range used by solution methods like the ACP. This idea is strongly supported by the results recently published by Varga et al. [31] who determined enthalpies of drop solution at 702 °C and enthalpies of formation from the binary oxides at 25 °C for zirconium tungstate and isostructural molybdates. Their results clearly show that the trigonal polymorphs are generally enthalpically more stable than the cubic phases. This explains why low-temperature solution methods yield t-ZrW_2O_8 [11,12] unless special conditions like topotaxy [32] or seeding [10] favour the formation of c-ZrW_2O_8.

From a structural point of view, trigonal and cubic zirconium tungstate polymorphs exhibit both strong common features and substantial differences [4,28]. The connectivity of coordination polyhedra is the same in both structures: Each [ZrO_6]-octahedron is corner-linked to six [WO_4]-tetrahedra, each [WO_4]-tetrahedron is corner-linked to only three [ZrO_6]-octahedra and has one terminal oxygen. Nevertheless, completely different structures are formed: In c-ZrW_2O_8, chains of alternating [ZrO_6]- and [WO_4]-polyhedra build an open framework structure, whereas in t-ZrW_2O_8 layers of connected [ZrO_6]- and [WO_4]-polyhedra are bonded by van der Waals forces. Thus, the long-range structure may be a dominant factor affecting the thermodynamic stability. Despite their common features, these two structures cannot be transformed into each other without the breaking of bonds and complete reconstruction. This may cause a kinetic hindrance for the transition of cubic to trigonal ZrW_2O_8, which is thermodynamically feasible but has not been observed so far [31]. Summing up, we find that neither phase-pure c-ZrW_2O_8 is directly accessible by the amorphous citrate process nor can t-ZrW_2O_8 be transformed to c-ZrW_2O_8 at low temperatures.

On the other hand, the short-range structural features common to both polymorphs should permit a very rapid conversion of t-ZrW_2O_8 into c-ZrW_2O_8 at temperatures within the thermodynamic stability range of the latter. Fig. 8 shows the X-ray diffractogram of a product resulting from up-quenching t-ZrW_2O_8 to 1125 °C, holding it at this temperature for 20 s and then quenching it down to room temperature. It is clearly visible that this procedure exclusively yields c-ZrW_2O_8. Fig. 9 presents the typical morphology of the c-ZrW_2O_8 powder. It can be seen that the formation of c-ZrW_2O_8 in its stability range leads to some sintering, but the particles remain relatively small (500 nm to 10 μm) because of the very short dwelling time at high temperature.

In order to evaluate the linear thermal expansion coefficient (CTE) of c-ZrW_2O_8 obtained by the procedure described

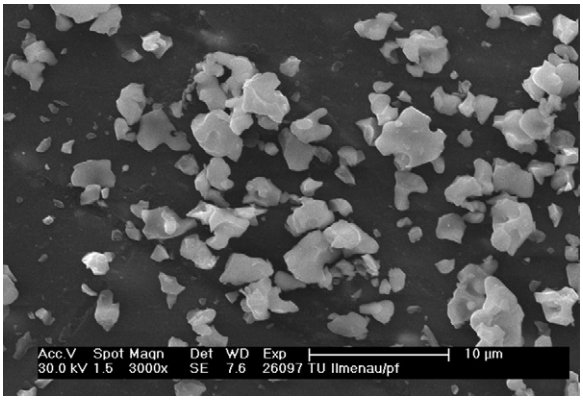

Fig. 9. SEM micrograph of c-ZrW_2O_8 made from t-ZrW_2O_8 (20 s 1125 °C).

above, the *d*-value of the 660 peak ($d_{6\,6\,0}$) was determined by variable temperature XRD in the range from 30°C to 120 °C. From the linear decrease of $d_{6\,6\,0}$ with increasing temperature we calculated a CTE of $-10.2 \times 10^{-6}\,K^{-1}$, which is in agreement with the results published by Hashimoto et al. [33,34].

4. Summary and conclusion

The results of our study show that the amorphous citrate process can be successfully applied to the system ZrO_2–WO_3, including the metastable compound ZrW_2O_8. The complex stability was found to be rather insensitive to variations of pH and molar ratio CA:metal. On the other hand, ionic crosslinking and, therefore, consistency and swelling behaviour of the gels largely depend on these variables. These gel properties, in turn, influence heat and mass transfer during gel thermolysis. Strong evidence of the formation of stable heterometallic Zr–W-citrate complexes comes from the fact that oxide crystallization from Zr–W-citrate gels occurred at a significantly higher temperature (740 °C) than from the corresponding monometallic gels (<500 °C). Using an optimized heating regime, phase separation into the binary oxides was avoided and phase-pure metastable trigonal zirconium tungstate was obtained. Though the amorphous citrate process enabled us to kinetically suppress the crystallization of the equilibrium phases ZrO_2 and WO_3, the desired cubic zirconium tungstate was not directly accessible. As with other low-temperature solution methods, the thermodynamically more stable trigonal polymorph crystallized. We finally succeeded in preparing phase-pure cubic zirconium tungstate by using the as-synthesized trigonal ZrW_2O_8 as an intermediate and up-quenching it to temperatures within the stability range of the cubic phase (1125 °C) for a very short time (<1 min). From a processing point of view, this technique based on the amorphous citrate process has the advantage that it makes use of only simple chemicals and laboratory procedures and that it offers much saving in processing time.

Acknowledgements

Financial support from the German Research Foundation (Collaborative Research Centre 622) is gratefully acknowledged. We would like to thank Dr. W. Schmitz of the University of Leipzig for performing variable temperature XRD measurements.

References

[1] A.K.A. Pryde, K.D. Hammonds, M.T. Dove, V. Heine, J.D. Gale, Origin of the negative thermal expansion in ZrW_2O_8 and ZrV_2O_7, J. Phys.: Condens. Matter 8 (1996) 10973–10982.
[2] M.G. Tucker, A.L. Goodwin, M.T. Dove, D.A. Keen, S.A. Wells, J.S.O. Evans, Negative thermal expansion in ZrW_2O_8: mechanisms, rigid unit modes and neutron total scattering, Phys. Rev. Lett. 95 (2005) 255501-1–255501-4.
[3] T.A. Mary, J.S.O. Evans, T. Vogt, A.W. Sleight, Negative thermal expansion from 0.3 to 1050 Kelvin in ZrW_2O_8, Science 272 (1996) 90–92.
[4] M. Auray, M. Quarton, Zirconium tungstate, Acta Cryst. C 51 (1995) 2210–2213.
[5] E. Niwa, S. Wakamiko, T. Ichikawa, S. Wang, T. Hashimoto, Preparation of dense ZrO_2/ZrW_2O_8 cosintered ceramics with controlled thermal expansion coefficients, J. Ceram. Soc. Jpn. 112 (2004) 271–275.
[6] L.M. Sullivan, C.M. Lukehart, Zirconium tungstate/polyimide nanocomposites exhibiting reduced coefficient of thermal expansion, Chem. Mater. 17 (2005) 2136–2141.
[7] L.L.Y. Chang, M.G. Scroger, B. Phillips, Condensed phase relations in the systems ZrO_2–WO_2–WO_3 and HfO_2–WO_2–WO_3, J. Am. Ceram. Soc. 50 (1967) 211–215.
[8] C. Closmann, A.W. Sleight, J.C. Haygarth, Low-temperature synthesis of ZrW_2O_8 and Mo-substituted ZrW_2O_8, J. Solid State Chem. 139 (1998) 424–426.
[9] U. Kameswari, A.W. Sleight, J.S.O. Evans, Rapid synthesis of ZrW_2O_8 and related phases, and structure refinement of $ZrWMoO_8$, Int. J. Inorg. Mater. 2 (2000) 333–337.
[10] C. Lind, A.P. Wilkinson, Seeding and the non-hydrolytic sol–gel synthesis of $ZrW_2O_8$and $ZrMo_2O_8$, J. Sol–Gel Sci. Technol. 25 (2002) 51–56.
[11] A.P. Wilkinson, C. Lind, S. Pattanaik, A new polymorph of ZrW_2O_8 prepared using nonhydrolytic sol–gel chemistry, Chem. Mater. 11 (1999) 101–108.
[12] L.D. Noailles, H.H. Peng, J. Starkovich, B. Dunn, Thermal expansion and phase formation of ZrW_2O_8 aerogels, Chem. Mater. 16 (2004) 1252–1259.
[13] C. Marcilly, P. Courty, B. Delmon, Preparation of highly dispersed mixed oxides and oxide solid solutions by pyrolysis of amorphous organic precursors, J. Am. Ceram. Soc. 53 (1970) 56–57.
[14] P. Courty, H. Ajot, C. Marcilly, Oxydes mixtes ou en solution solide sous forme tres divisee obtenus par decomposition thermique de precursors amorphes, Powder Technol. 7 (1973) 21–38.
[15] M. Kakihana, M. Yoshimura, Synthesis and characteristics of complex multicomponent oxides prepared by polymer complex method, Bull. Chem. Soc. Jpn. 72 (1999) 1427–1443.
[16] J.P. Jolivet, Metal Oxide Chemistry and Synthesis. From Solution to Solid State, John Wiley and Sons, Chichester, 1994, p. 141.
[17] J.J. Cruywagen, L. Krüger, E.A. Rohwer, Complexation of tungsten (VI) with citrate, J. Chem. Soc., Dalton Trans. 7 (1991) 1727–1731.
[18] J. Choy, Y. Han, Citrate route to the piezoelectric Pb(Zr, Ti)O_3 oxide, J. Mater. Chem. 7 (1997) 1815–1820.
[19] G. Kickelbick, U. Schubert, Hydroxy carboxylate substituted oxozirconium clusters, J. Chem. Soc., Dalton Trans. 8 (1999) 1301–1305.
[20] Y. Narendar, G.L. Messing, Mechanisms of phase separation in gel-based synthesis of multicomponent metal oxides, Catal. Today 35 (1997) 247–268.
[21] K. de Buysser, P.F. Smet, B. Schoofs, E. Bruneel, D. Poelman, S. Hoste, I. van Driessche, Aqueous sol–gel processing of precursor oxides for ZrW_2O_8 synthesis, J. Sol–Gel Sci. Technol. 43 (2007) 347–353.
[22] M.S.G. Baythoun, F.R. Sale, Production of strontium-substituted lanthanum manganite perovskite powder by the amorphous citrate process, J. Mater. Sci. 17 (1982) 2757–2769.
[23] A.E. Martell, R.M. Smith, Critical Stability Constants, vol. 5: First Supplement, Plenum Press, New York, 1982, p. 329.
[24] J. Berger, M. Reist, J.M. Mayer, O. Felt, N.A. Peppas, R. Gurny, Structure and interactions in covalently and ionically crosslinked chitosan hydrogels for biomedical applications, Eur. J. Pharm. Biopharm. 57 (2004) 19–34.
[25] Powder Diffraction File, Release 2004, International Centre for Diffraction Data (ICDD), 2004.
[26] P. Karen, A. Kjekshus, Citrate-gel syntheses in the Y(O)–Ba(O)–Cu(O) system, J. Am. Ceram. Soc. 77 (1994) 547–552.
[27] Y. Narendar, G.L. Messing, Kinetic analysis of combustion synthesis of lead magnesium niobate from metal carboxylate gels, J. Am. Ceram. Soc. 80 (1997) 915–924.
[28] S. Allen, R.J. Ward, M.R. Hampson, R.K.B. Gover, J.S.O. Evans, Structures and phase transitions of trigonal $ZrMo_2O_8$ and $HfMo_2O_8$, Acta Cryst. B 60 (2004) 32–40.
[29] PowderX, Institute of Physics, Chinese Academy of Sciences, Beijing.
[30] K. van Werde, D. Mondelaers, G. Vanhoyland, D. Nelis, M.K. van Bael, Thermal decomposition of the ammonium zinc acetate citrate precursor for aqueous chemical solution deposition of ZnO, J. Mater. Sci. 37 (2002) 81–88.

[31] T. Varga, C. Lind, A.P. Wilkinson, H. Xu, C.E. Lesher, A. Navrotsky, Heats of formation for several crystalline polymorphs and pressure-induced amorphous forms of AMo_2O_8 (A=Zr,Hf) and ZrW_2O_8, Chem. Mater. 19 (2007) 468–476.

[32] M.S. Dadachov, R.F. Howe, R.M. Lambrecht, EXAFS study of the local structure of zirconium tungstate and molybdate biomedical gel generators, Radiochim. Acta 86 (1999) 51–60.

[33] T. Hashimoto, T. Katsube, Y. Morito, Observation of two kinds of phase transitions of ZrW_2O_8 by power-compensated differential scanning calorimetry and high-temperature XRD, Solid State Commun. 116 (2000) 129–132.

[34] T. Hashimoto, Y. Morito, Thermal analysis of phase transition in negative-thermal-expansion oxide ZrW_2O_8, J. Ceram. Soc. Jpn. 110 (2002) 823–825.